

## INVESTIGATION OF THE MECHANISMS OF LOCAL AMORPHIZATION IN A HEAVILY DOPED CRYSTALLINE SEMICONDUCTOR $n$ -TiNiSn

V.A. ROMAKA<sup>1,2</sup>, YU.V. STADNYK<sup>3</sup>, D. FRUCHART<sup>4</sup>, V.V. ROMAKA<sup>3</sup>, P. ROGL<sup>5</sup>, V.M. DAVYDOV<sup>3</sup>, YU.K. GORELENKO<sup>3</sup>, A.M. GORYN<sup>3</sup>

UDC 621.315  
©2008

<sup>1</sup>Ya. Pidstryhach Institute of Applied Problems of Mechanics and Mathematics, Nat. Acad. Sci. of Ukraine  
(3b, Naukova Str., Lviv 79060, Ukraine),

<sup>2</sup>National University "Lvivs'ka Politehnika"  
(1, Knyaz Roman Str., Lviv 79005, Ukraine; e-mail: vromaka@polymet.lviv.ua),

<sup>3</sup>Ivan Franko Lviv National University  
(6, Kyryl and Mephodii Str., Lviv 79005, Ukraine),

<sup>4</sup>Laboratoire de Cristallographie, CNRS  
(BP 166, Grenoble 38042, Cedex 9, France; e-mail: daniel.fruchart@grenoble.cnrs.fr),

<sup>5</sup>Institute of Physical Chemistry, Vienna University  
(A-1090, Vienna, Austria; e-mail: peter.franz.rogl@univie.ac.at)

The calculations of the electronic density of states (DOS) and structural parameters for  $n$ -TiNiSn intermetallic semiconductor heavily doped with an In acceptor impurity ( $N_A^{\text{In}} \approx 9.5 \times 10^{19} \div 1.9 \times 10^{21} \text{cm}^{-3}$ ) are performed. The temperature and concentration dependences of resistivity, thermoelectric coefficient, magnetic susceptibility, and X-ray structural characteristics are experimentally studied. The structurally disordered local regions and the presence of fluctuations of the continuous energy bands in  $\text{TiNiSn}_{1-x}\text{In}_x$  are revealed.

for Ni [8]. The donor impurity was introduced in  $p$ -TiCoSb by means of the substitution of Ni for Co [9]. For the first time for the given class of semiconductors, the authors of papers [7–9] specified the dominating mechanisms of electric conduction, stressed the role of the impurity bands in the determination of conductivity over wide concentration and temperature intervals, and formulated the conditions for the appearance of maximal values of the thermoelectric power factor  $Z^*$  [10].

### 1. Introduction

The paper presents the results of studies of the influence of the high-level doping with an In acceptor impurity ( $N_A^{\text{In}} \approx 10^{19} \div 10^{21} \text{cm}^{-3}$ ) on the structure, energy, and electrokinetic and magnetic characteristics, as well as on the electronic DOS of the intermetallic semiconductor  $n$ -TiNiSn. Along with obtaining the practical results related to promising thermoelectric materials of the MgAgAs structural type [1–6], the aim of the investigations was the search for the correlation between the impurity concentration and the structural perfectness of the semiconductor and its electrokinetic and magnetic properties.

In works [7–9], the peculiar features of the influence of a high-level doping of intermetallic semiconductors with acceptor and/or donor impurities were studied. In particular, the acceptor impurity was introduced in  $n$ -ZrNiSn through a substitution of Sc for Zr [7] and Co

For the materials under investigation, the synthesis process is characterized by the peculiar features which give rise to the fulfillment of the conditions for obtaining the partially disordered crystalline structures, i.e. those with a local amorphization. In particular, such conditions include a high level of doping ( $N_A, N_D \approx 10^{19} \div 10^{21} \text{cm}^{-3}$ ) [12] and the fast cooling after the melting [11]. In its turn, the local amorphization leads to the fluctuations of the continuous energy bands, which, particularly, manifest themselves in that the activation energies deduced from the temperature dependence of resistivity ( $\varepsilon_1^\rho$ ) and the thermopower coefficient ( $\varepsilon_1^\alpha$ ) are different from each other within the same temperature range. Such a difference was revealed earlier in  $\text{ZrNiSn}_{1-x}\text{In}_x$  [13]. However, the authors didn't provide the experimental evidence for the local amorphization of the crystalline semiconductor. In this work, such results are presented for the  $n$ -TiNiSn.

At present, contrary to the case of the theory of hopping conductivity [14], the theory of thermoelectric power for the region of hopping conductivity is far from being completed. Therefore, the experimental studies of

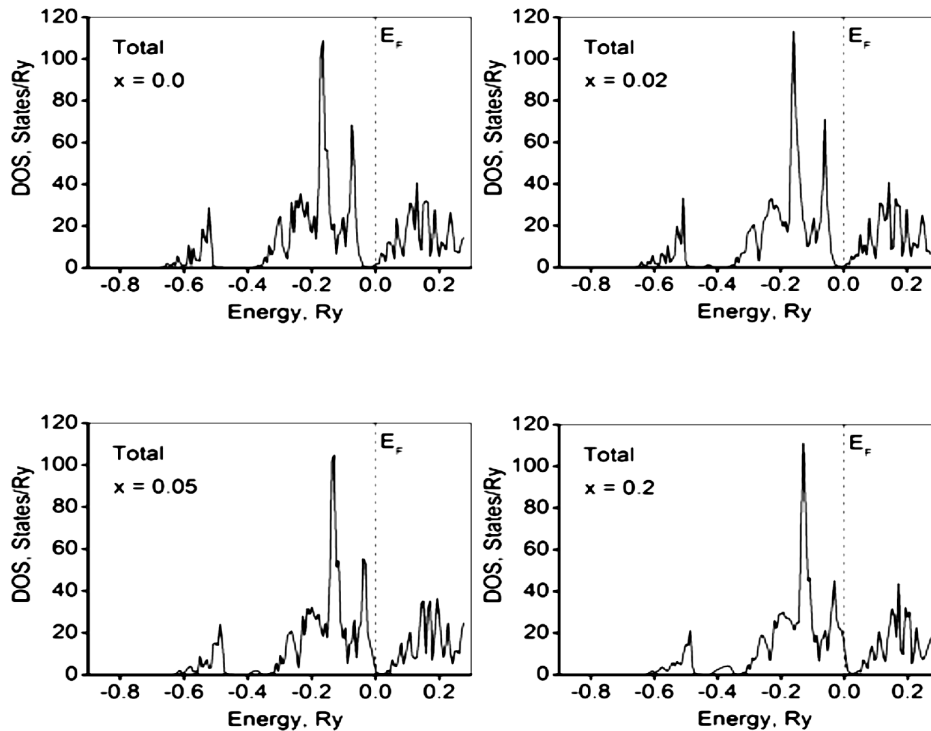


Fig. 1. DOS distribution for four specimens of  $\text{TiNiSn}_{1-x}\text{In}_x$

the energy characteristics of heavily doped and compensated semiconductors can stimulate the theoretical studies.

The features of a specimens' fabrication method as well as the details of structural studies, measurements of resistivity, thermoelectric coefficient (with respect to copper), and magnetic susceptibility (the Faraday method) over the temperature range 80–380 K are presented in work [7]. The technique of calculations of the DOS (the KKR-CPA-LDA method) is described in [15].

## 2. Calculations of Electronic Structure of $\text{TiNiSn}_{1-x}\text{In}_x$

While calculating the DOS distribution, we assumed that the crystalline structure of the alloys is ordered, i.e. all atoms occupy the positions imposed by the MgAgAs structure type. The crystalline potential and the electron charge density were chosen to be spherically symmetric inside a sphere and invariable within an intermediate region (the muffin-tin method). In intermetallic semiconductors of the MgAgAs structure type, only three of four possible atomic positions with the  $\bar{4}3m$  symmetry are filled. To increase the packing density

of a Wigner–Seitz cell, we introduced an additional empty sphere around the fourth unoccupied position. For the non-overlapping spheres, the radii were chosen in such way that the maximal filling of a Wigner–Seitz cell would be achieved. The calculations of the total DOS, as well as individual partial contributions from various atoms and electronic shells with  $l_{\text{max}} = 2$ , were carried out. The procedure of self-consistency was performed until a difference between values of the potential reached  $10^{-4}$  Ry.

The calculation results (Fig. 1) for the undoped  $\text{TiNiSn}$  specimen coincide with those obtained earlier (see [16]) and show that  $\text{TiNiSn}$  is a semiconductor, in which the energy gap between the conduction and valence bands is a result of a strong hybridization of the  $d$ -states of transition metals (Ti and Ni). The electron DOS of the conduction band is mainly determined by the  $d$ -states of Ti, whereas the valence band is formed by the  $d$ -states of Ni which are overlapped with the  $d$ -states of Ti and  $p$ -states of Sn. The Fermi level  $\varepsilon_F$  is located in the band gap near the bottom of the conduction band. In experiment, this feature should manifest itself in the negative sign of the thermoelectric coefficient.

The doping of  $\text{TiNiSn}$  with the In acceptor impurity leads to a drift of the Fermi level towards the valence

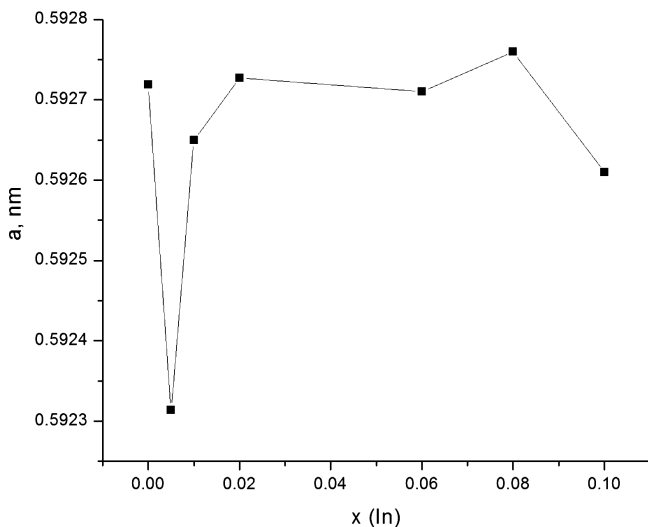


Fig. 2. Unit cell parameter  $a$  as a function of  $x$  for the  $\text{TiNiSn}_{1-x}\text{In}_x$  specimens

band, with the energy gap value being invariable. The calculations show that, as soon as  $x$  goes over 0.05, the Fermi level crosses the mobility edge of the valence band, which should result, in turn, in the sign reversal of the thermoelectric coefficient. The further increase in the impurity concentration is accompanied by the entry of  $\varepsilon_F$  into the valence band and its drift in the band.

### 3. Structural Studies of $\text{TiNiSn}_{1-x}\text{In}_x$

The X-ray phase, structure, and microprobe analyses confirmed that all the  $\text{TiNiSn}_{1-x}\text{In}_x$  specimens under investigation are single-phase, and the distribution of atoms in them corresponds to the MgAgAs structural type: 4Ni in 4(c) 1/4 1/4 1/4; 4Sn in 4(a) 0 0 0; 4Ti in 4(b) 1/2 1/2 1/2. For each of the specimens, we refined the crystalline structure with the use of a Siemens D5000 X-ray diffractometer and WinCSD software [17] and determined a unit cell period  $a$ .

It is known that, for an ordered crystalline structure, a gradual substitution of one kind of atoms by another one brings about the monotonic changes in the unit cell parameter and intensities of the X-ray Bragg reflections. It is clear that such a substitution will also affect the interplane distances  $d$  and this change is also expected to be gradual. However, as a substitution level for the main component is low enough (less than 5 at. %), the resultant change in  $d$  turns out to be negligible, since the diffraction peak consists of the almost indiscernible set of reflections characterized by different  $d$  values. In

this case, the parameters of a reflection peak of a certain order, namely the peak intensity and the full width at a half maximum (FWHM), reflect the integral distribution of interplane distances. At the same time, it is FWHM that is very sensitive to the structural transformations of a unit cell, originating from a substitution of the components of a solid solution [18].

The analysis of changes in the unit cell parameter for the  $\text{TiNiSn}_{1-x}\text{In}_x$  specimens shows the following. For the low-level In doping ( $0 \leq x \leq 0.005$ ), the increase in  $x$  results in the period diminution (Fig. 2). As  $x$  changes from 0.005 to 0.02, the period increases and approaches the value characteristic of the undoped semiconductor. The further growth in  $x$  leads to negligible changes in the period for  $0.02 \leq x \leq 0.08$  and its further increase with  $x$  for  $x > 0.08$ . A similar behavior of the  $a(x)$  dependence, namely the presence of a dip, was also observed in  $\text{ZrNiSn}_{1-x}\text{In}_x$  [13]. It is difficult to explain such a result by considering only a single-act substitution, either In for Sn or In for Ti, since the In atomic radius  $r_{\text{In}}$  is greater than the radius of each of the  $\text{TiNiSn}$  components ( $r_{\text{In}} = 1.66\text{\AA}$ ,  $r_{\text{Ti}} = 1.46\text{\AA}$ ,  $r_{\text{Sn}} = 1.58\text{\AA}$ ,  $r_{\text{Ni}} = 1.24\text{\AA}$ ), and, thus, such a kind of substitution should lead to an increase in the unit cell parameter.

The combined analysis of the FWHM and the peak amplitude for X-ray Bragg reflections shows that the local amorphization, i.e. a partial mutual substitution of Ti and Sn atoms, is already characteristic of the undoped  $\text{TiNiSn}$  specimen. Figure 3 demonstrates a non-monotonous dependence of the peak half-widths and intensities for some of the reflections for a series of  $\text{TiNiSn}_{1-x}\text{In}_x$  specimens on  $x$ . It should be noted that it is impossible to present all the available information on the FWHM changes and possible variants of the atom mutual substitutions due to a restricted volume of this paper. Figure 3 gives only some idea of a possible mechanism. For example, the decrease in the peak intensity and the increase in the FWHM of 002 reflection in the range of  $x = 0 \div 0.02$  along with a diminution of the unit cell period indicate that the substitution of Sn by smaller atoms occurs. It is Ti atoms that are prime candidates, but also Ni atoms cannot be excluded.

The peak amplitude depends on the kind of a scattering atom. So, the X-ray scattering factor  $R_{\text{In}} \approx R_{\text{Sn}} > R_{\text{Ti}}$ . As follows from Fig. 3, the In doping of  $\text{TiNiSn}$  leads to the complex structural changes in almost all crystallographic planes formed by Ti atoms and (Sn,In) ones. This analysis leads to the conclusion that the initial non-doped structure of  $\text{TiNiSn}$  is partially disordered (the intensities of 111 and 002 reflections are

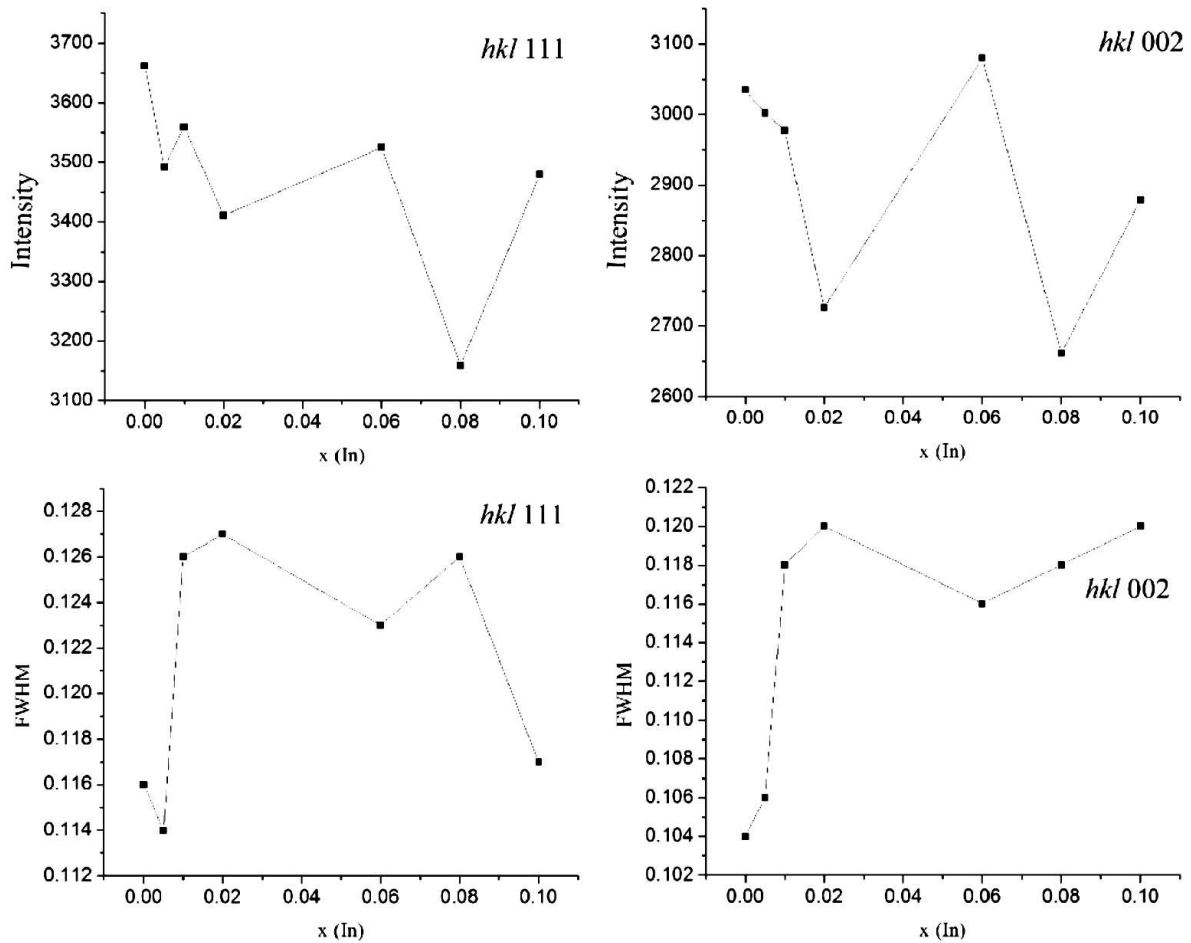


Fig. 3. FWHM and relative intensity  $I$  of the  $hkl$  Bragg reflections as a function of  $x$  for the  $\text{TiNiSn}_{1-x}\text{In}_x$  specimens

greater than that characteristic of the compounds doped with In). This finding is in compliance with the results of the analysis of interplane distances and with the conclusion about a local amorphization of the crystalline compounds under study. For this reason, the correct chemical formula for the solid solution should be written as  $\text{Ti}_{1-y}\text{Ni}(\text{Sn}_{1-x}\text{In}_x)_y$ .

#### 4. Electrokinetic and Magnetic Characteristics of $\text{TiNiSn}_{1-x}\text{In}_x$

As follows from Fig. 4, the high-temperature activation regions are characteristic of the  $\ln \rho$  vs  $1/T$  and  $\alpha$  vs  $1/T$  dependences for all the specimens. For some of them, however, the activation regions are also observed at low temperatures. A general picture is as follows. In a parent  $n$ -TiNiSn specimen, the low-temperature activation region is not observed,

and the conductance is of metallic character. The doping of  $n$ -TiNiSn with the compensating In impurity results in the breakdown of metallicity and the appearance of low-temperature activation regions for  $x = 0.005$  and  $0.02$ . The further increase in the In concentration restores the metallic type of conductance.

The activation energies  $\varepsilon_1^\rho$  and  $\varepsilon_1^\alpha$ , deduced from the high-temperature regions of the  $\ln \rho$  vs  $1/T$  and  $\alpha$  vs  $1/T$  dependences, are shown in the Table. The value of  $\varepsilon_1^\alpha$  was calculated with the use of the Mott expression for the thermoelectric coefficient [11]

$$\alpha = \frac{k_B}{e} \left( \frac{\varepsilon}{k_B T} - \gamma + 1 \right) \quad (1)$$

under the assumption that  $\gamma = 1$ . As in the case of  $\text{ZrNiSn}_{1-x}\text{In}_x$  [13], the values of  $\varepsilon_1^\rho$  and  $\varepsilon_1^\alpha$  substantially

differ from one another, which yields, with regard for the local amorphization of specimens, the presence of the fluctuations of the continuous energy bands.

The doping of  $n$ -TiNiSn with the In impurity up to the concentrations corresponding to  $x = 0.02$  increases the compensation degree of the semiconductor and leads to a drift of the Fermi level away from the mobility edge of the conduction band [19]. An experimental proof of this process, predicted by calculations, consists in the growth of the activation energies  $\varepsilon_1^p$  and  $\varepsilon_1^\alpha$  (see table).

A negative sign of the thermoelectric coefficient characteristic of the whole temperature range for the concentrations  $x = 0 \div 0.02$  (Figs. 4 and 5) implies that the overcompensation phenomenon doesn't occur in TiNiSn $_{1-x}$ In $_x$  (in ZrNiSn $_{1-x}$ In $_x$ , the compensation was observed at  $x = 0.02$  [13]). But even at higher concentrations of the impurity,  $\alpha(x)$  doesn't change its sign. This result contradicts that obtained from the calculations. Let us analyze this point in more details.

The TiNiSn $_{1-x}$ In $_x$  specimens are the Pauli paramagnets. As a result of this fact, the DOS at the Fermi level is proportional to the magnetic susceptibility of the electron gas ( $n(\varepsilon_F) \sim \chi$ ). Mott assumed that, in a doped compensated semiconductor, when the energy states at the Fermi level are localized, the sign of the thermoelectric coefficient also depends on whether the DOS in the vicinity of  $\varepsilon_F$  increases or decreases as a function of energy:

$$\alpha = \frac{k_B}{e} \frac{W^2}{2k_B T} \left. \frac{\partial \ln n(\varepsilon)}{\partial \varepsilon} \right|_{\varepsilon=\varepsilon_F}, \quad (2)$$

where  $W$  is the hopping conductivity energy [11]. In the case where the compensation level is less than 1/2, the impurity band of the  $p$ -type, for example, gives the thermoelectric coefficient characteristic of the  $n$ -type band.

The decrease in the values of  $\alpha(x)$  and  $\chi(x)$  within the region  $x = 0 \div 0.005$  is understandable and can be explained by the reduction in the DOS at the Fermi level as a result of the change in the compensation degree of the  $n$ -type semiconductor upon the introduction of an

#### The concentrational and energy characteristics for TiNiSn $_{1-x}$ In $_x$

Specimen number	$x$	$N_A$ , cm $^{-3}$	$\varepsilon_1^p$ , meV	$\varepsilon_1^\alpha$ , meV	$\varepsilon_3^p$ , meV	$\varepsilon_3^\alpha$ , meV
20	0	0	16.9	19.5	–	3.7
36	0.005	$9.5 \times 10^{19}$	69.6	89.7	1.9	1.9
38	0.02	$3.8 \times 10^{20}$	96.7	93.4	1.4	1.7
40	0.06	$1.1 \times 10^{21}$	115.6	126.0	–	0.3
41	0.08	$1.5 \times 10^{21}$	94.7	114.2	–	0.05
42	0.1	$1.9 \times 10^{21}$	52.5	61.6	–	–

acceptor impurity. The minima observed on the  $\alpha(x)$  and  $\chi(x)$  dependences ( $x \approx 0.02$ ,  $T = 80$  K) and the increase in the values of magnetic susceptibility and conductivity with the further growth of the impurity concentration testify to the beginning of the rise in the DOS at the Fermi level. By analogy with [13], it is such a kind of behavior that is expected when  $\varepsilon_F$  crosses the middle of the energy gap and drifts towards the valence band. The decrease in the carrier activation energy  $\varepsilon_1^p$  from the Fermi level to the mobility edge of the valence band, which is observed in the compositional range  $x = 0.06 \div 0.1$ , is in compliance with the theoretical calculations and can be served as a proof of the mentioned fact. This phenomenon is accompanied by a decrease in the  $\alpha(x)$  value.

However, the sign of the thermoelectric coefficient keeps unchangeable for both cases, either the decrease ( $x < 0.02$ ) or increase ( $x > 0.02$ ) in the DOS at the Fermi level. This means that the semiconductor conductance is of the electron type. For this reason, the Mott's conclusion is not valid in our case.

In our opinion, the following explanation is more correct. Earlier, we provided the evidence for the presence of local amorphization in TiNiSn $_{1-x}$ In $_x$  specimens. However, when calculating the distribution of the electron DOS, a choice of a Wigner–Seitz cell was made proceeding from the assumption that the atomic arrangement is ordered. The actual picture essentially differs from that used in calculations, since the doping of the intermetallic compound TiNiSn with In doesn't simply result in the introduction of the acceptor with respect to Sn atoms. While introducing In atoms, we, without wishing to do this, initiate a complex mechanism of partial mutual substitutions for almost all atomic positions of Ti and (Sn, In). These mutual substitutions, which take part, in turn, in the formation of both the valence and conduction bands, give rise to the rearrangement of the electron DOS, which makes it different from what we expected. The numerical calculations show the non-monotonous changes in the values of the band gap and the DOS at the Fermi level, as well as the drift of  $\varepsilon_F$  towards the valence or conduction band. At certain combinations of the atomic arrangements within the Wigner–Seitz cell, the band gap disappears. Such a variety of the results is a reflection of the multivariant arrangement of atoms in a unit cell of the TiNiSn $_{1-x}$ In $_x$  solid solution. It is worth to note that the structural studies show only the dynamics of the atomic position change, but the information on precise atomic locations can only be obtained from the results of neutron diffraction studies.

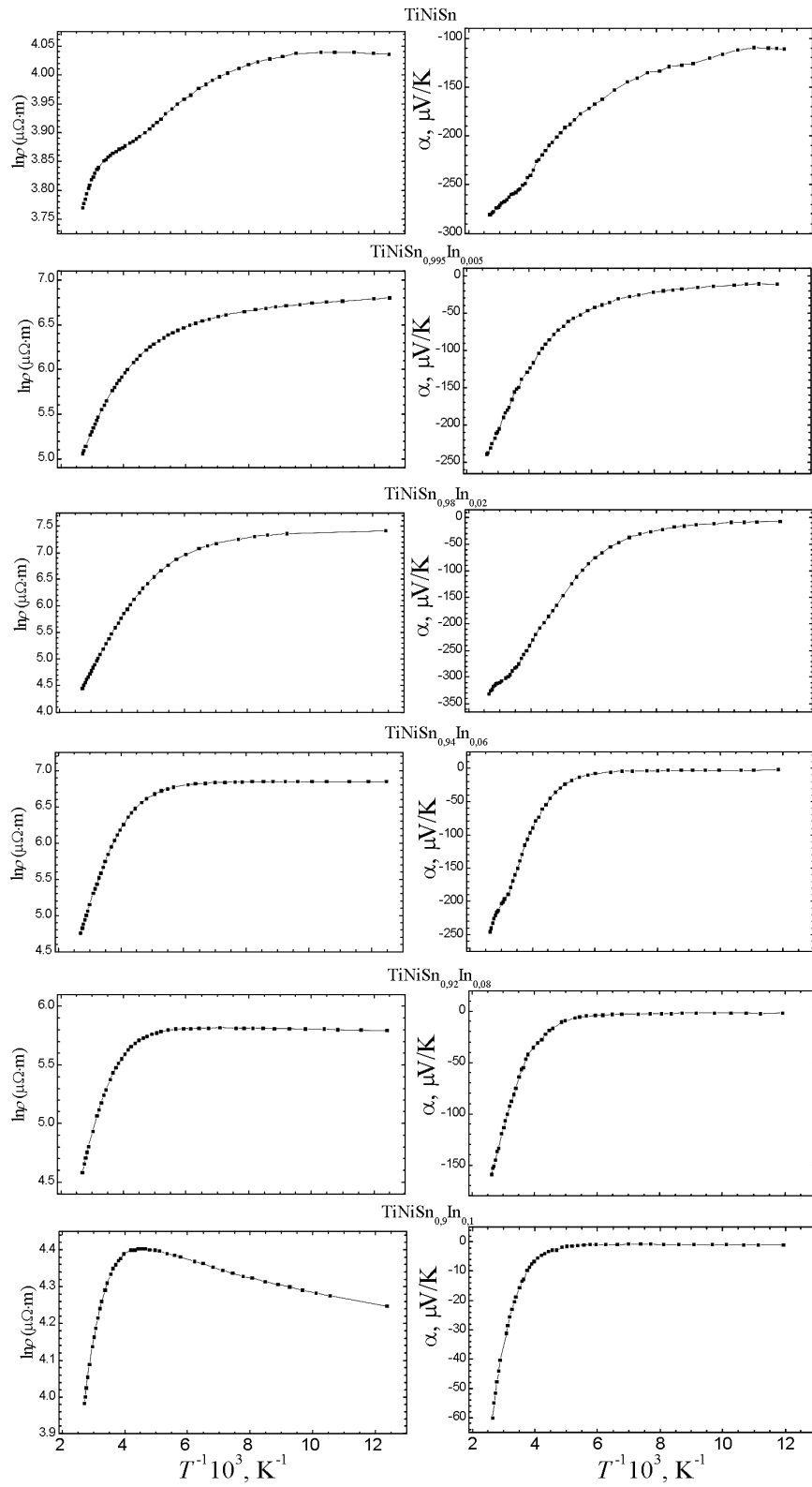


Fig. 4. Temperature dependences of resistivity  $\rho$  and thermoelectric coefficient  $\alpha$  for  $\text{TiNiSn}_{1-x}\text{In}_x$

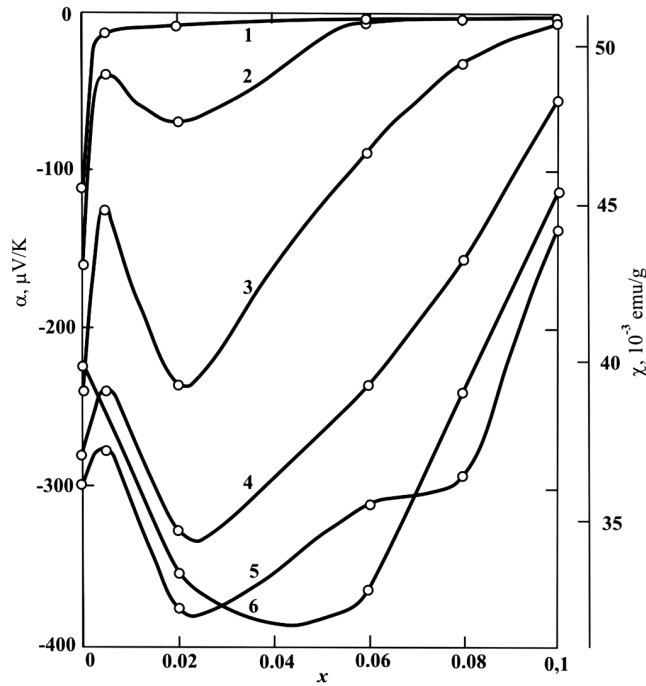


Fig. 5. Concentration dependences of the thermoelectric coefficient  $\alpha$  at 80 (1), 160 (2), 250 (3), and 370K (4) and the magnetic susceptibility  $\chi$  at 300 (5) and 80K (6)

Thus, the introduction of the In impurity into TiNiSn cannot unambiguously be interpreted as the introduction of the acceptor with respect to Sn. This statement would be correct if In simply substituted for Sn. As this is not the case, it can be assumed that, for the specimens under investigation, the negative sign of the thermoelectric coefficient is a result of the strong reduction of the band gap and the non-monotonous change of the compensation degree of the semiconductor due to its partial amorphization.

For the specimens which display the low-temperature activation regions on the  $\alpha(x)$  and  $\chi(x)$  dependences, we also calculated the activation energies  $\varepsilon_3^p$  and  $\varepsilon_3^g$  (see the Table). The presence of such activation regions at low temperatures testifies to that the electron hopping over the states which are close to the Fermi level also contributes to the semiconductor conductance, as a result of the drift of  $\varepsilon_F$  away from the mobility edge of the conductivity band (the small-scale fluctuations of the conductivity band become isolated [12]). In the Shklovskii–Efros model, such a drift is equivalent to a lowering of the temperature and should be accompanied by a reduction of the hopping conductance energy  $\varepsilon_3^p$  [14]. As follows from the Table,  $\varepsilon_3^p$  diminishes when the

impurity concentration grows in the range  $x = 0.005 \div 0.02$ . What is more, it is also seen that the amplitude of small-scale fluctuations  $\varepsilon_3^g$  decreases upon the growth of  $x$  up to 0.08. At the same time, the energy of the hopping conductance  $\varepsilon_3^p$  is reduced with decrease in the amplitude of small-scale fluctuations. At  $N \geq 5.7 \times 10^{20} \text{cm}^{-3}$  ( $x \geq 0.06$ ), the depth of small-scale fluctuations becomes negligible ( $\varepsilon_3^g(x = 0.06) = 0.3 \text{ meV}$ ), and the hopping conductivity is no longer observed, since the majority carriers “fill in” small-scale fluctuations.

## 5. Conclusions

In summary, the doping of the *n*-TiNiSn intermetallic semiconductor with the In impurity is accompanied by complex structural transformations and changes in the semiconductor compensation degree, the DOS at the Fermi level, and the band gap. The doping of the *n*-TiNiSn with the In impurity up to the concentrations, which correspond to the compositions of  $\text{TiNiSn}_{1-x}\text{In}_x$  with  $x \leq 0.02$ , leads to a rise in the fluctuation amplitude  $\varepsilon_1^\alpha$ , the energy distance between the Fermi level and the mobility edge  $\varepsilon_1^p$ , and also to a decrease in the depth of small-scale fluctuations  $\varepsilon_3^g$ . As  $x$  exceeds 0.02, the DOS at the Fermi level increases, and the hopping conductivity disappears due to the smallness of the amplitude of small-scale fluctuations.

The work is performed within the frames of the grants of the National Academy of Sciences of Ukraine (No. 0106U000594) and the Ministry of Science and Education of Ukraine (No. 0106U001299 and No. 0106U005498).

1. F.G. Aliev, N.B. Brandt, V.V. Kozyr'kov *et al.*, *Pis'ma Zh. Eksp. Teor. Fiz.* **45**, 535 (1987).
2. S. Bhattacharya, A.L. Pope, R.T. Littleton *et al.*, *Appl. Phys. Lett.* **77**, 2476 (2000).
3. Y. Kawaharada, K. Kurosaki, H. Muta *et al.*, *J. Alloys Comp.* **381**, 9 (2004).
4. S. Katsuyama, H. Matsushima, and M. Ito, *J. Alloys Comput.* **385**, 232 (2004).
5. C. Uher, J. Yang, S. Hu *et al.*, *Phys. Rev. B* **59**, 8615 (1999).
6. A. Slebarski, A. Jezierski, A. Zygmunt *et al.*, *Phys. Rev. B* **57**, 9544 (1998).
7. V.A. Romaka, Yu.V. Stadnyk, M.G. Shelyapina *et al.*, *Fiz. Tekhn. Polupr.* **40**, 136 (2006).
8. V.A. Romaka, M.G. Shelyapina, Yu.K. Gorenko *et al.*, *Fiz. Tekhn. Polupr.* **40**, 676 (2006).
9. V.A. Romaka, M.G. Shelyapina, Yu.V. Stadnyk *et al.*, *Fiz. Tekhn. Polupr.* **40**, 796 (2006).
10. V.A. Romaka, D. Fruchart, M.G. Shelyapina *et al.*, *Fiz. Tekhn. Polupr.* **40**, 1309 (2006).

11. N.F. Mott, *Metal-Insulator Transitions* (Taylor & Francis, London, Bristol, 1990).
12. B.I. Shklovskii and A.L. Efros, *Zh. Exp. Teor. Fiz.* **61**, 816 (1971).
13. V.A. Romaka, Yu.V. Stadnyk, D. Fruchart *et al.*, *Fiz. Tekhn. Polupr.* **41**, 1059 (2007).
14. B.I. Shklovskii, *Fiz. Tekhn. Polupr.* **7**, 112 (1973).
15. H. Akai, *J. Phys.: Condens. Matter.* **1**, 8045 (1989).
16. J. Tobola and J. Pierre, *J. Alloys Comp.* **296**, 243 (2000).
17. L.G. Akselrud, Yu.N. Grin, P.Y. Zavalij *et al.*, in *12th European Crystallographic Meeting: Collected Abstracts* (Nauka, Moscow, 1989).
18. H. Lipson and H. Steeple, *Interpretation of X-ray Powder Diffraction Patterns* (St. Martin's Press, New York, 1970).
19. B.I. Shklovskii and A.L. Efros, *Zh. Eksp. Teor. Fiz.* **62**, 1156 (1972).

Received 11.04.07

Translated from Ukrainian by A.I. Tovstolytkin

ДОСЛІДЖЕННЯ МЕХАНІЗМУ ЛОКАЛЬНОЇ  
АМОРФІЗАЦІЇ СИЛЬНОЛЕГОВАНОГО  
КРИСТАЛІЧНОГО НАПІВПРОВІДНИКА  
 $n$ -TiNiSn

*В.А. Ромака, Ю.В. Стадник, Д. Фрушарт, В.В. Ромака,  
П. Рогол, В.М. Давидов, Ю.К. Гореленко, А.М. Горинь*

## Резюме

Виконано розрахунок розподілу електронної густини (DOS) та структурних параметрів, досліджено температурні та концентраційні залежності питомого опору, коефіцієнта термо-ерс, магнітної сприйнятливості та рентгеноструктурні характеристики інтерметалічного напівпровідника  $n$ -TiNiSn, сильнолегованого акцепторною домішкою In ( $N_A^{\text{In}} \approx 9,5 \cdot 10^{19} \div 1,9 \cdot 10^{21} \text{ см}^{-3}$ ). Виявлено локальні структурні неупорядкування та наявність флуктуацій зон неперервних енергій  $\text{TiNiSn}_{1-x}\text{In}_x$ .